

# Digraph Signal Processing with Generalized Boundary Conditions

Bastian Seifert and Markus Püschel

**Abstract**—Signal processing on directed graphs (digraphs) is problematic, since the graph shift, and thus associated filters, are in general not diagonalizable. Furthermore, the Fourier transform in this case is now obtained from the Jordan decomposition, which may not be computable at all for larger graphs. We propose a novel and general solution for this problem based on matrix perturbation theory: We design an algorithm that adds a small number of edges to a given digraph to destroy nontrivial Jordan blocks. The obtained digraph is then diagonalizable and yields, as we show, an approximate eigenbasis and Fourier transform for the original digraph. We explain why and how this construction can be viewed as generalized form of boundary conditions, a common practice in signal processing. Our experiments with random and real world graphs show that we can scale to graphs with a few thousands nodes, and obtain Fourier transforms that are close to orthogonal while still diagonalizing an intuitive notion of convolution. Our method works with adjacency and Laplacian shift and can be used as preprocessing step to enable further processing as we show with a prototypical Wiener filter application.

**Index Terms**—Graph signal processing, graph Fourier transform, directed graph, matrix perturbation theory

## I. INTRODUCTION

Signal processing on graphs (GSP) extends traditional signal processing (SP) techniques to data indexed by vertices of graphs and has found many real world applications, including in analyzing sensor networks [1], the detection of neurological diseases [2], gene regulatory network inference [3], 3D point cloud processing [4], and rating prediction in video recommendation systems [5]. See also [6] for a recent overview.

For undirected graphs there are two major variants of GSP that differ in the chosen shift (or variation) operator: one is based on the Laplacian [7], the other is based on the adjacency matrix [8]. Both are symmetric and thus diagonalizable with an associated orthogonal Fourier transform. Since the definition of the shift is sufficient to derive a complete, basic SP toolset [9] one obtains in both cases meaningful (but different) notions of spectrum, frequency response, low and high frequencies, Parseval identities, and other concepts.

However, in many applications the graph signals are associated with directed graphs (digraphs). Examples include argumentation framework analysis [10], predatory-prey patterns [11], big data functions [12], social networks [13], and epidemiological models [14]. In these cases the GSP frameworks become problematic since non-symmetric matrices may not be diagonalizable. A natural replacement is to use the Jordan normal form (JNF) for the spectral decomposition of

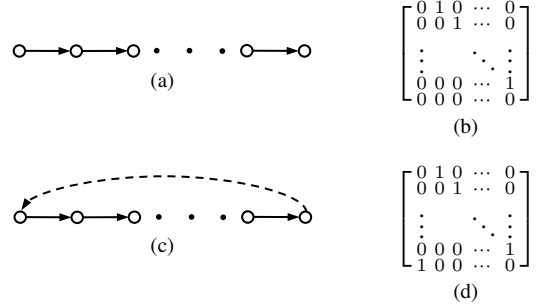


Fig. 1: The most natural graph model for a finite-duration discrete time signal (a) yields the non-decomposable shift matrix in (b). Adding one edge (c) yields the well-known circular shift (d) and DFT-based spectral analysis. This edge makes the support a circle, which is equivalent to assuming the signal as periodic.

the graph [15]. But the JNF is known to be numerically highly unstable [16] and thus not easy to compute or, for larger graphs, not computable at all. Further, spectral components have now dimensions larger than one, since no eigenbasis is available, which complicates the application of SP methods. In the theory of graph neural networks the non-diagonalizability of digraphs is problematic as well [17].

In this paper we propose a novel, practical solution to this problem. The basic idea is to generalize, in a sense, the well-known concept of boundary conditions to arbitrary digraphs to make them diagonalizable. It is best explained using finite discrete-time SP as motivating example.

**Motivating example.** Imagine we are trying to build an SP framework for discrete finite-duration time signals using GSP. The most natural solution is the graph shown in Fig. 1a: it captures the operation of the time shift and includes no assumptions on the behavior of the signal to the left and to the right of its support. The associated shift matrix is shown in Fig. 1b: it is a single Jordan block and thus, in a sense, a worst case: it has only the eigenvalue 0, a one-dimensional eigenspace, and cannot be diagonalized, not even into block-diagonal form.

Indeed, Fig. 1a is not the model commonly adopted but instead Fig. 1c, which adds one edge usually interpreted as a circular boundary condition. Adding this edge (in GSP) makes the graph a circle, and hence signals on this graph are equivalent to periodic signals in DSP. The associated shift matrix describes the well-known circular shift (Fig. 1d). It has an eigendecomposition with distinct eigenvalues, done by the discrete Fourier transform (DFT). Note that in almost

all applications that use the DFT, *the signal is not really periodically extended outside its support*. So, in a sense, adding the extra edge, or assuming periodicity, can be viewed as an assumption used to obtain a workable basic SP toolset.

There are a few other aspects worth noting. First, the added edge is the unique single edge that makes the matrix in Fig. 1b diagonalizable and invertible. Further, the eigenvectors of the cyclic shift matrix are approximate eigenvectors of the matrix in Fig. 1b, and the DFT diagonalizes this matrix approximately (namely up to a rank-one matrix). We will study these and other aspects in our contribution.

**Contributions.** The overall contribution of this paper is a novel approach to make GSP practical on non-diagonalizable digraphs. For a given digraph, our high-level idea is to add a small number of edges to make the graph diagonalizable (and also invertible and with distinct eigenvalues if desired) to obtain a practical form of spectral analysis. To achieve this we leverage results from perturbation theory [18] on the destruction of Jordan blocks by adding low-rank matrices.

First, we instantiate the perturbation theory to the GSP setting and use it to design an algorithm that iteratively destroys Jordan blocks by adding edges. We investigate the consequences for spectral analysis and show that the added edges can be considered as generalized boundary conditions in the sense that they add periodic boundary conditions on subgraphs and increase the number of cycles in the graph. Second, we provide an efficient implementation of our algorithm that employs additional techniques to make it numerically feasible and scalable to large graphs. In particular, the graph Fourier basis we obtain is numerically stable by construction.

We apply our algorithm to various synthetic and real world graphs showing that usually few edges suffice and that we can process even difficult graphs with a few thousand nodes or close to being acyclic. Finally, we include an application example of a graph Wiener filter enabled by our approach.

**Related work.** The non-diagonalizability in digraph SP is an important open problem [6, Sec. III.A] and a number of solutions have been proposed. Most approaches aim for a notion of Fourier basis that circumvents JNF computation at the price of other GSP properties that are lost.

One idea is to define a different notion of Fourier basis that is orthonormal by construction. Motivated by the Lovász extension of the graph cut size, [19] defines a notion of directed total variation and constructs an orthonormal Fourier basis that minimizes the sum of these. Extending these ideas, [20], [21] defines a digraph Fourier basis as the solution of an optimization problem on the Stiefel manifold, minimizing a dispersion function to evenly spread frequencies in the frequency range. Both approaches only work for real signals and yield real Fourier transforms, though a slight modification of the approach was used in [21] to make the connection to the circle graph in standard discrete time signal processing. In both cases there is no intuitive notion of convolution in the graph domain anymore, i.e., all filtering now requires the Fourier transform.

Another idea is an approximation of the Fourier basis that almost diagonalizes the adjacency matrix by allowing small, bounded off-diagonal entries as proposed in [22]. The

approach is based on the Schur decomposition and the authors solve a non-convex optimization problem to obtain a numerically stable basis that can be inverted to compute the Fourier transform. The approach could be problematic for acyclic digraphs which have zero as the only eigenvalue.

The work in [23], [24], [25] maintains the idea of Jordan decomposition but alters the definition of the graph Fourier transform to decompose into Jordan subspaces only, instead of a full JNF. This way a coordinate-free definition of Fourier transform is obtained, which fulfills a generalized Parseval identity. A method for the inexact, but numerical stable, computation of this graph Fourier transform was proposed in [24].

Another approach is to change the graph shift operator and thus change the underlying definitions of spectrum and Fourier transform. In [26] the Hermitian Laplacian matrix is proposed, which is always diagonalizable. The known directed Laplacian was used in [27] and a scaled version of it, with a detailed study, in [28]. Both shifts are not diagonalizable, and our proposed method is applicable in both cases.

The work in [29] stays within the framework of [8] but identifies the subset of filters that are diagonalizable. Since these form a subalgebra, they are generated by one element which can be used as diagonalizable shift at the price of a smaller filter space. The approach fails for digraphs with all eigenvalues being zero, i.e., directed acyclic graphs.

Certain very regular digraphs possess orthonormal Fourier transforms, e.g., those associated with a directed hexagonal lattice [30] or the directed quincunx lattice [31].

Our approach computes an approximate Fourier basis and transform as some prior work, but is fundamentally different in that it does so by adding a small number of edges to achieve both: stay within the traditional GSP setting and maintain an intuitive notion of convolution.

## II. GRAPH SIGNAL PROCESSING

In this section we recall the theory of signal processing on graphs, and, in particular, directed graphs (digraphs). We focus on digraphs without edge weights as these are most prone to non-diagonalizable adjacency matrices. However, our approach is applicable to weighted digraphs and discussed later.

**Directed graphs.** A digraph  $G = (\mathcal{V}, \mathcal{E})$  consists of a set of  $n$  vertices  $\mathcal{V}$  and a set of edges  $\mathcal{E} \subseteq \mathcal{V} \times \mathcal{V}$ . Assuming a chosen ordering of the vertices,  $\mathcal{V} = (v_1, \dots, v_n)$ , a digraph can be represented by its  $n \times n$  adjacency matrix  $A$  with entries

$$A_{i,j} = \begin{cases} 1 & \text{if } (v_i, v_j) \in \mathcal{E}, \\ 0 & \text{else.} \end{cases} \quad (1)$$

We consider graphs with loops, i.e., edges of the form  $(v_i, v_i)$  are allowed. If  $A$  is symmetric, i.e.,  $(v_i, v_j) \in \mathcal{E}$  implies  $(v_j, v_i) \in \mathcal{E}$ , the digraph can be viewed as an undirected graph, and hence  $A$  is diagonalizable. For other digraphs this may not be the case.

**Graph signal.** A graph signal  $s$  on  $G$  associates values with the vertices, i.e., it is a mapping of the form

$$s : \mathcal{V} \rightarrow \mathbb{C}; v_i \mapsto s_i. \quad (2)$$

Using the chosen vertex ordering, the graph signal is represented by the vector  $s = (s_i)_{1 \leq i \leq n} \in \mathbb{C}^n$ .

**Fourier transform based on adjacency matrix.** In GSP based on [15], the Jordan decomposition of  $A$ ,

$$A = V \cdot J \cdot V^{-1}, \quad (3)$$

where  $J$  is in Jordan normal form (JNF), yields  $\mathcal{F} = V^{-1}$  as the graph Fourier transform of the graph. The graph Fourier transform of a graph signal  $s$  is

$$\hat{s} = \mathcal{F}s. \quad (4)$$

The frequencies are ordered by total variation, defined as

$$\text{TV}_A(v) = \|v - \frac{A}{|\lambda_{\max}|}v\|_1, \quad (5)$$

where  $\lambda_{\max}$  is the eigenvalue of  $A$  with largest magnitude.

Note that the computation of the JNF is numerically unstable [16]. For example,  $\begin{bmatrix} 0 & 1 \\ 0 & 0 \end{bmatrix}$  is in JNF, whereas  $\begin{bmatrix} \epsilon & 1 \\ 0 & -\epsilon \end{bmatrix}$  is diagonalizable for every  $\epsilon \neq 0$ . Thus symbolic computation is needed, which, however, becomes too expensive for graphs with hundreds or more nodes.

**Fourier transform based on Laplacian.** An alternative approach to GSP is based on the Laplacian of a graph. For digraphs, several variants of Laplacians have been proposed including the most common directed Laplacian [32], the normalized Laplacian [28], the random-walk Laplacian [33], or the magnetic Laplacian [34]. The last two variants are always diagonalizable, as they are either symmetric or Hermitian.

In [7] the graph Fourier transform for undirected graphs was defined using the eigendecomposition of the Laplacian. For the extension of this framework to directed graphs, [27] thus uses the directed Laplacian

$$L = D - A, \quad (6)$$

where  $D$  is the diagonal matrix of either in- or out-degrees. The Jordan decomposition of the directed Laplacian

$$L = V \cdot J \cdot V^{-1}, \quad (7)$$

is then used to define the graph Fourier transform  $\mathcal{F} = V^{-1}$  as before. The frequencies are ordered in [27] by graph total variation as well.

Our focus will be GSP based on (3) but we will also instantiate our approach to GSP based on (7) to which it is equally applicable.

### III. GENERALIZED BOUNDARY CONDITIONS FOR DIGRAPHS

In the introduction we gave a motivating example for the contribution in this paper: a "bottom-up" explanation of the cyclic boundary condition (or, equivalently, periodicity) inherently assumed with DFT-based spectral analysis.<sup>1</sup> Namely, in GSP terms, the cyclic boundary condition is the minimal addition of edges to the graph in Fig. 1a to obtain a proper spectrum with distinct eigenvalues.

<sup>1</sup>More common is what one could call the "top-down" explanation for periodicity, which naturally arises, for example, when sampling the spectrum of continuous signals.

In this section we extend this basic idea and construction to arbitrary digraphs: Given a digraph, our goal is to add the minimal number of edges that make the digraph diagonalizable. In matrix terms this means adding to the adjacency matrix  $A$  a low-rank adjacency matrix  $B$  containing the additional edges, such that  $A+B$  is diagonalizable. The same technique can be used to make  $A$  also invertible or the eigenvalues distinct. An analogous construction can be done for the directed Laplacian by ensuring that the Laplacian structure is preserved.

Our approach builds on results from matrix perturbation theory on the destruction of Jordan blocks under low-rank changes of a matrix.

We first introduce the needed results from perturbation theory and then instantiate them in the GSP setting to design an algorithm that destroys Jordan blocks by adding edges to graphs. We provide a number of theoretical results and explain in which way one may consider the added edges as generalized boundary conditions. Accompanying the theory we provide small, illustrating examples.

#### A. Results from Perturbation Theory

We recall some terminology. For a matrix  $M$ ,  $v$  is a right eigenvector if  $Mv = \lambda v$  and  $u$  a left eigenvector if  $u^T M = \lambda u^T$ , i.e.,  $u$  is an eigenvector of the transpose  $M^T$ .  $M$  and  $M^T$  have the same JNF.

Let  $J = V^{-1}MV$  be in JNF. Then  $J$  is a block-diagonal matrix consisting of Jordan blocks of the form

$$\begin{bmatrix} \lambda & 1 & 0 & \dots & 0 \\ 0 & \lambda & 1 & \dots & 0 \\ \vdots & & \ddots & & \vdots \\ 0 & 0 & 0 & \dots & 1 \\ 0 & 0 & 0 & \dots & \lambda \end{bmatrix} \quad (8)$$

where  $\lambda$  is an eigenvalue. Each eigenvalue can have multiple such blocks and of different size. The Jordan basis (columns of  $V$ ) associated with each block includes exactly one right eigenvector, which is in first position of the block, and exactly one left eigenvector (a row in  $V^{-1}$ ), which is in last position.

**Matrix perturbation and Jordan blocks.** Our work builds on results by Moro and Dopico [18] that study the effect on the Jordan blocks when perturbing a given matrix  $M \in \mathbb{C}^{n \times n}$  by adding a low rank matrix  $B$ . The following is the main result that we will use. It can also be found in [35], [36], but we work with the exposition in [18] in a slightly adapted formulation.

*Theorem 1 ([18])* Assume the different sizes of the Jordan blocks to a given eigenvalue  $\lambda$  of  $M$  are  $f_1 > f_2 > \dots > f_t$  and that the Jordan blocks are ordered accordingly. Let  $r_s$  be the number of blocks of size  $\geq f_s$ ,  $s = 1, \dots, t$ , and set  $r_0 = 0$ . For each  $r_s$  denote the associated left and right eigenvectors (one per block) with  $u_k^T$  and  $v_k$ ,  $k = 1, \dots, r_s$ . Let  $B$  be a matrix of rank  $\rho$ , with  $r_{s-1} < \rho \leq r_s$  and define

$$\Phi_s = \begin{bmatrix} u_1^T \\ \vdots \\ u_{r_s}^T \end{bmatrix} B \begin{bmatrix} v_1 & \dots & v_{r_s} \end{bmatrix} \in \mathbb{C}^{r_s \times r_s}. \quad (9)$$

We denote with  $\Phi_{s-1}$  the upper-left block of dimension  $r_{s-1}$  of  $\Phi_s$ .  $\Phi_0$  is considered as the empty submatrix. If

$$\sum_{\substack{\phi \\ \phi \text{ principal } \rho \times \rho \text{ submatrix} \\ \text{of } \Phi_s \text{ containing } \Phi_{s-1}}} \det(\phi) \neq 0, \quad (10)$$

then the Jordan blocks of  $M + B$  for  $\lambda$  are those of  $M$  minus the  $\rho$  largest ones. A principle submatrix is obtained by deleting rows and columns with the same indices.

If real or complex matrices are concerned then a random matrix  $B$  will satisfy (10) for all eigenvalues with probability 1. This so-called generic case was the purpose of the study in [18]. In our case, neither the matrices  $M$  nor the desired  $B$  (to add edges) are generic since they have only entries 0 or 1 and thus constitute finite sets.

Note that the condition in the theorem is sufficient but not necessary. Further, (10) is a statement about the Jordan blocks to one eigenvalue and does not state what happens to Jordan blocks of other eigenvalues, which can be destroyed as well (generic case), or remain untouched, or even be enlarged.

In general, destroying a Jordan block for  $\lambda$  yields new eigenvalues and the basis for the JNF also changes when adding  $B$  to  $M$ .

Theorem 1 allows the destruction of all Jordan blocks to one eigenvalue with a properly chosen  $B$ , but the condition is complex. Thus later, we prefer to do so iteratively, one block at a time, with matrices  $B$  of rank  $\rho = 1$ . This means all  $\phi$  in (10) have size  $1 \times 1$ , which avoids determinant computations for simplicity and better numerical stability. The following corollary considers this special case. Note that  $\rho = 1$  implies that  $s = 1$  such that  $0 = r_0 < \rho \leq r_1$ .

*Corollary 2* For a given eigenvalue  $\lambda$  of  $M$  let  $u_1, \dots, u_{r_1}$  be the left and  $v_1, \dots, v_{r_1}$  be the right eigenvectors of the Jordan blocks of the largest size  $f_1$ . Let  $B$  be a matrix of rank 1. If

$$\sum_{k=1}^{r_1} u_k^T B v_k \neq 0, \quad (11)$$

then adding  $B$  to  $M$  destroys one of the largest Jordan blocks to  $\lambda$  of  $M$ .

**PROOF:** In this special case of Theorem 1 we have  $\rho = 1 \leq r_1$ . The principle  $1 \times 1$  submatrices  $\phi$  of

$$\Phi_1 = \begin{bmatrix} u_1^T \\ \vdots \\ u_{r_1}^T \end{bmatrix} B \begin{bmatrix} v_1 & \dots & v_{r_1} \end{bmatrix}$$

containing the empty matrix  $\Phi_0$  correspond exactly to the diagonal elements of  $\Phi_1$ , which yields the result.  $\square$

Fig. 1b is a very simple example since it is already in JNF with only one Jordan block. The right eigenvector for the block is  $u_1 = [1, 0, \dots, 0]^T$  and the left eigenvector is  $v_1 = [0, 0, \dots, 1]$ . The matrix  $B$  containing the added edge in position  $(n, 1)$  indeed satisfies (10):

$$[0, 0, \dots, 1] \cdot B \cdot [1, 0, \dots, 0]^T = 1, \quad (12)$$

and is the only matrix  $B$  adding one edge with this property.

**Behavior of new eigenvalues.** The following result shows how the eigenvalues change under a rank-one perturbation. It can be easily proved using the matrix determinant lemma but is not practical for large scale graphs.

*Lemma 3* Let  $B = ab^T$  be a rank-one matrix. Then the new eigenvalues of the perturbed matrix  $M + B$  are the solutions to the equation

$$b^T (xI - M)^{-1} a = 1. \quad (13)$$

The left-hand side is a rational function, hence the eigenvalues are given by the roots of a polynomial.

For the example in Fig. 1, (13) becomes  $1/x^n = 1$ , i.e., the new eigenvalues are exactly the  $n$ th roots of unity, as expected.

The literature also provides bounds on the distance between old and new (under low-rank perturbation) eigenvalues (e.g., [37, Thm. 8]), but we found them to be loose and not of practical value in our application scenario.

Finally, [38, Thm. 6.2] shows that for real or complex matrices, in the generic case,  $M + B$  has no repeated eigenvalues, which are not already eigenvalues of  $M$ .

### B. Adding Edges to Destroy Jordan blocks

Our goal is to perturb a directed graph by adding edges to destroy the Jordan blocks of its adjacency matrix and Corollary 2 will be our main tool. First, we establish the viability of this approach, meaning it is always possible to find a matrix  $B$  adding one edge that satisfies (11).

In the following, we use the column-wise vectorization of a matrix  $B \in \mathbb{C}^{m \times n}$ :  $\text{vec}(B) = (b_{1,1}, \dots, b_{m,1}, b_{1,2}, \dots, b_{m,n})^T$ . Vectorization satisfies  $\text{vec}(ABC) = (C^T \otimes A) \text{vec}(B)$  for matrices of compatible dimensions, where  $\otimes$  is the Kronecker product.

*Theorem 4* Adding or deleting one edge is sufficient to destroy the largest Jordan block of an adjacency matrix for a chosen eigenvalue  $\lambda$ .

**PROOF:** Let  $u_1, \dots, u_r$  and  $v_1, \dots, v_r$  be the left and right eigenvectors of the largest Jordan blocks for the eigenvalue  $\lambda$ , respectively. Then (11) can be written as

$$\begin{aligned} 0 &\neq \sum_{k=1}^r u_k^T B v_k \\ &= \sum_{k=1}^r \text{vec}(u_k^T B v_k) = \left( \sum_{k=1}^r v_k^T \otimes u_k^T \right) \text{vec}(B). \end{aligned}$$

Since the  $u_k$  and the  $v_k$  are linear independent, the same holds for the set of the  $v_k \otimes u_k$ . Thus,  $w^T = \sum_{k=1}^r v_k^T \otimes u_k^T$  is a nonzero row vector and for an adjacency matrix it is enough (and always possible) to set exactly one entry (which depends on the  $u_k$  and  $v_k$ ) of  $B$  to 1 to ensure that the result is nonzero. The number of nonzero elements in  $w$  is the number of choices. If for each choice,  $A$  already contains the edge, we can instead delete an edge, choosing  $-1$  as entry in  $B$ .  $\square$

It is not possible to strengthen the hypothesis to destroying Jordan blocks by only adding edges in each case. A counter example is the complete graph, which, however, has only

```

function DESTROYALLJORDANBLOCKS( $A$ )
  while  $A$  not diagonalizable do
     $u_1, \dots, u_r \leftarrow$  left EVs to largest Jordan blocks
     $v_1, \dots, v_r \leftarrow$  right EVs to largest Jordan blocks
    if  $\exists (i, j)$  s.t.  $\sum_k u_{k,j} v_{k,i} \neq 0$  and  $A_{i,j} = 0$  then
       $A_{i,j} \leftarrow 1$ 
    else
      select  $(i, j)$  random s.t.  $A_{i,j} = 0$ 
       $A_{i,j} \leftarrow 1$ 
    end if
  end while
  return  $A$ 
end function

```

Fig. 2: The mathematical algorithm to obtain a diagonalizable digraph.  $u_{k,j}$  is the  $j$ th element of  $u_k$ .

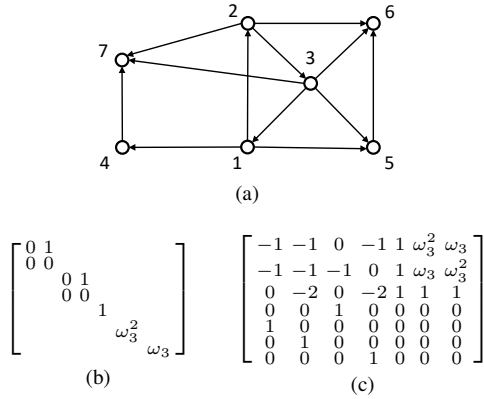


Fig. 3: The graph shown in (a) has the Jordan normal form  $J = V^{-1}AV$  shown in (b). The matrix  $V$  of generalized eigenvectors is shown in (c), with  $\omega_3 = \exp(-2\pi j/3)$ .

Jordan blocks of size 1. In our experiments with (the most relevant) sparse graphs, we never encountered the case that a Jordan block could not be destroyed by adding an edge.

**Basic algorithm.** Using Theorem 10 we can formulate the basic mathematical algorithm to make a digraph adjacency matrix  $A$  diagonalizable by adding edges (Fig. 2). The algorithm is iterative, adding one edge in each step as described in Theorem 10,  $A \rightarrow A + B$ , to destroy the largest Jordan block.  $B$  has only one entry 1. Note that in the case that all edges that are eligible for adding already exist in the graph, we choose to add a random edge instead of removing an edge. This way the algorithm is guaranteed to terminate as discussed below.

For a practical implementation, various additional details need to be considered that we discuss later.

**An example.** To illustrate Alg. 2 we provide a detailed example.

*Example 5* We consider the graph in Fig. 3, which has the characteristic polynomial  $p(x) = x^4(x^3 - 1)$  and two Jordan blocks of size 2 for eigenvalue 0. We apply Alg. 2. The right eigenvectors for the Jordan blocks of size two are the first and third column of  $V$ :

$$\begin{aligned} v_1 &= [-1 \ -1 \ 0 \ 0 \ 1 \ 0 \ 0]^T, \\ v_2 &= [0 \ -1 \ 0 \ 1 \ 0 \ 0 \ 0]^T. \end{aligned} \quad (14)$$

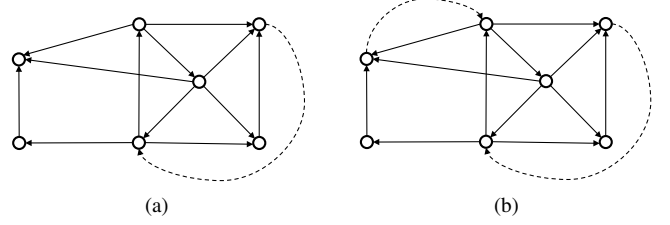


Fig. 4: The modified graph with the first (a) and second (b) edge added by the proposed abstract algorithm.

The corresponding left eigenvectors are the second and fourth row of  $V^{-1}$ :

$$\begin{aligned} u_1^T &= [0 \ 0 \ 0 \ 0 \ 0 \ 1 \ 0], \\ u_2^T &= [0 \ 0 \ 0 \ 0 \ 0 \ 0 \ 1]. \end{aligned} \quad (15)$$

Thus (10) takes the form

$$0 \neq u_1^T B v_1 + u_2^T B v_2 = -b_{6,1} - b_{6,2} + b_{6,5} - b_{7,2} + b_{7,4}, \quad (16)$$

and we have five choices. We choose  $b_{6,1} = 1$ , as shown in Fig. 4a, which defines  $B$ .

Note the effect on the JNF (Fig. 3b) when  $B$  is added:  $V^{-1}(A + B)V = J + V^{-1}BV$  with

$$V^{-1}BV = \begin{bmatrix} 0 & 0 & 0 & 0 & 0 & 0 & 0 \\ -1 & -1 & 0 & -1 & 1 & \omega_3^2 & \omega_3 \\ 0 & 0 & 0 & 0 & 0 & 0 & 0 \\ 0 & 0 & 0 & 0 & 0 & 0 & 0 \\ -\frac{4}{3} & -\frac{4}{3} & 0 & -\frac{4}{3} & \frac{4}{3} & \frac{4}{3}\omega_3^2 & \frac{4}{3}\omega_3 \\ -\frac{1}{3} & -\frac{1}{3} & 0 & -\frac{1}{3} & \frac{1}{3} & \frac{1}{3}\omega_3^2 & \frac{1}{3}\omega_3 \\ -\frac{1}{3} & -\frac{1}{3} & 0 & -\frac{1}{3} & \frac{1}{3} & \frac{1}{3}\omega_3^2 & \frac{1}{3}\omega_3 \end{bmatrix}. \quad (17)$$

The addition of this matrix to the Jordan form of  $A$  modifies all eigenvalues, except for the remaining Jordan block for eigenvalue 0.

For the remaining Jordan block for eigenvalue 0 in the modified graph, the right and left eigenvectors are given, respectively, by

$$v_2 = [0 \ -1 \ 0 \ 1 \ 0 \ 0 \ 0]^T, \quad u_2^T = [0 \ 0 \ 0 \ 0 \ 0 \ 0 \ 1].$$

Condition (10) takes the form

$$u_2^T B v_2 = -b_{7,2} + b_{7,4}. \quad (18)$$

We add the edge  $b_{7,2} = 1$  and obtain the graph in Fig. 4b. The characteristic polynomial is now  $p(x) = x^7 - x^5 - 4x^4 - x^3 - 2x^2 - 1$ , which yields pairwise different eigenvalues (Fig. 5).

### C. Further Properties and Discussion

We discuss various properties of our basic algorithm, the results it produces, and further extensions. In particular, we provide an explanation for terming the added edges generalized boundary conditions.

**Minimal number of edges.** Theorems 10 and 1 give an immediate lower bound for the number of edges to destroy all Jordan blocks: it is the maximal number of Jordan blocks of size larger than one over all eigenvalues. The bound is then achieved if destroying this maximum number of blocks happens to destroy the Jordan blocks of all other eigenvalues

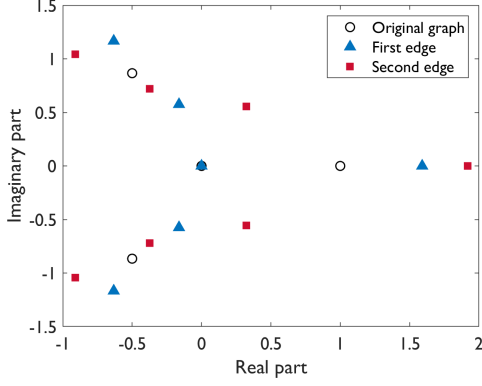


Fig. 5: The eigenvalues of the original graph on 7 nodes (black circles), after the first edge was added (blue triangles), and after the second edge was added (red squares).

as well. For real and complex matrices, this would hold in the generic case. For adjacency matrices, in general, it does not.

A trivial upper bound is the number of edges needed to make the graph symmetric. This is of course not the purpose of our work, a large number, and not the type of edges found by our algorithm in practice.

**Termination.** The algorithm in Fig. 2 always terminates since it adds an edge in every step, either one which destroys one Jordan block or a random one. In the worst case it would reach the unweighted complete graph, which is diagonalizable. Again, we note that in our extensive experiments on sparse graphs we never saw the case of a random edge, i.e., in every step a Jordan block got destroyed. Note that the potential (non-generic) case that a new Jordan block is created if another is destroyed thus also poses no problem for termination.

**Invertible adjacency matrix.** Since the adjacency matrix is considered as shift in the GSP of [8], it may be desirable that it is invertible. Our algorithm can be used for this purpose by also destroying all Jordan blocks for the eigenvalue zero, including those of size one.

**Approximate eigenvectors and Fourier transform.** Our algorithm takes as input an adjacency matrix  $A$  and outputs a diagonalizable  $A + B$ , where  $B$  contains all the added edges, say  $k$  many. As we show now, the eigenvectors of  $A + B$  are, in a sense, approximate eigenvectors of  $A$  and the same holds for the Fourier transform of  $A + B$ .

**Lemma 6** If  $v$  is an eigenvector of  $A + B$  to the eigenvalue  $\lambda$  then

$$\|Av - \lambda v\|_0 \leq k, \quad (19)$$

where  $\|\cdot\|_0$  is the  $\ell_0$ -pseudonorm that counts the entries  $\neq 0$ .

**PROOF:** Let  $I$  be the index set of zero rows of  $B$ ,  $|I| \geq n - k$ . Then

$$(Av)_{i \in I} = ((A + B)v)_{i \in I} = (\lambda v)_{i \in I} = \lambda(v)_{i \in I},$$

as  $B$  has no effect on the entries corresponding to  $I$ .  $\square$

As a consequence,  $A$  also gets diagonalized approximately by the Fourier transform  $\mathcal{F}$  of  $A + B$  in the following sense.

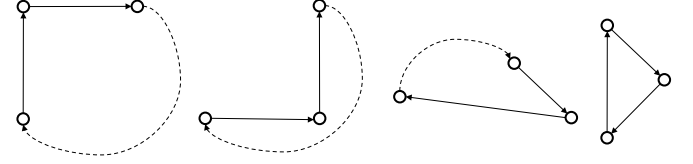


Fig. 6: The 4 subgraphs in  $\mathcal{H}_3$  of the graph in Fig. 4b. The added edges are dotted.

**Lemma 7** If  $\mathcal{F}(A + B)\mathcal{F}^{-1} = D$  (diagonal), then

$$\mathcal{F}A\mathcal{F}^{-1} = D - \mathcal{F}B\mathcal{F}^{-1},$$

is diagonal up to a matrix of rank  $k$ .

For example, the DFT diagonalizes the matrix in Fig. 1b up to a dense rank-one matrix, which is the outer product of the last column of DFT with the first row of  $\text{DFT}^{-1}$ .

**New edges as generalized boundary conditions.** We explain why the edges added by our algorithm to destroy Jordan blocks may be considered as generalized boundary conditions. In the example in Fig. 1 we saw that the added edge created a cycle. Intriguingly, this observation generalizes: there is an intrinsic relationship between diagonalizability (and invertibility) of  $A$  and the occurrence of cycles.

To do so, we first need the following theorem for digraphs that explains the connection between the coefficients of the characteristic polynomial of  $A$  and the simple cycles of the graph. We recall that a cycle is simple if all the vertices it contains are different. Further,  $H$  is called a subgraph of  $G$  if it contains a subset of the vertices and edges of  $G$ .

**Theorem 8 ([39])** Let  $G$  be a graph and denote by  $\mathcal{H}_i$  the set of all subgraphs of  $G$  with exactly  $i$  vertices and consisting of a disjoint union of simple directed cycles (equivalently,  $\mathcal{H}_i$  consists of all subgraphs with  $i$  nodes, each of which has indegree and outdegree = 1). Then the coefficients of the characteristic polynomial of  $G$

$$p_G(x) = x^n + a_{n-1}x^{n-1} + \dots + a_0 \quad (20)$$

have the form

$$a_i = \sum_{H \in \mathcal{H}_{n-i}} (-1)^{c(H)}, \quad (21)$$

where  $c(H)$  is the number of cycles  $H$  consists of.

For example the graph in Fig. 4b has four subgraphs on three vertices consisting of simple cycles shown in Fig. 6. Hence, by Theorem 8, its characteristic polynomial has the term  $-4x^4$ , which is indeed the case.

It is clear that adding edges cannot reduce the number of cycles in a graph. Theorem 8 implies that if an added edge is not part of any cycle, it will not change the characteristic polynomial. But Algorithm 2 does. Hence we get the following corollary.

**Corollary 9** Each edge that Algorithm 2 adds to a graph to destroy a Jordan block introduces additional simple cycles.

The added edges by Algorithm 2 thus add periodic boundary conditions to certain subgraphs (see the example in Fig. 6). Thus we term them generalized boundary conditions.

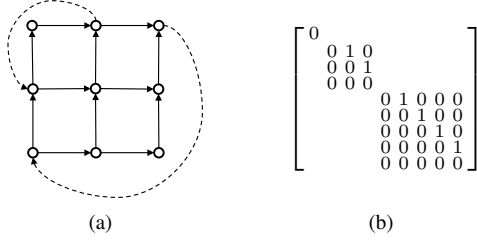


Fig. 7: The directed grid in (a) is an example of a directed acyclic graph with the JNF shown in (b). One possibility to destroy all Jordan blocks is adding both dashed edges (8, 4) and (9, 1).

One could consider vertices with indegree or outdegree = 0 (sources or sinks) as boundaries. Such vertices make  $A$  non-invertible, i.e., produce eigenvalues = 0. Our algorithm can be used to remove the eigenvalue 0 by adding edges, thus making  $A$  invertible and removing sinks and sources. Note that the added edges in Fig. 4b achieved exactly that.

**Directed acyclic graphs.** The class of directed acyclic graphs (DAGs) without self-loops constitutes in a sense the worst-case class for signal processing on graphs. A DAG represents a partial order, and thus the vertices can be topologically sorted to make  $A$  triangular, i.e., the characteristic polynomial is  $p(x) = x^n$  and the only eigenvalue is 0. Equivalently, no edge is part of a cycle and thus, by Theorem 8, all edges can be removed without changing  $p(x)$ , which yields the same result  $p(x) = x^n$ .

As an example consider the product graph of two directed path graphs in Fig. 7, which is a DAG. The vertices are numbered from 1 to 9 starting in the bottom left. The JNF consists of three Jordan blocks of sizes one, three, and five. Applying the proposed algorithm yields the condition to destroy the largest Jordan block as

$$6b_{9,1} \neq 0, \quad (22)$$

while the condition to destroy the second Jordan block is

$$\frac{1}{2}(b_{6,2} - b_{6,4} - b_{8,2} + b_{8,4}) \neq 0. \quad (23)$$

Hence adding the edge (9, 1) and any of the ones occurring in (23) makes the graph diagonalizable with distinct eigenvalues. One solution is shown in Fig. 7. Adding one more edge, which can be obtained from the condition

$$\frac{1}{3}(b_{3,3} - b_{3,5} + b_{3,7} - b_{5,3} + b_{5,5} - b_{5,7} + b_{7,3} - b_{7,5} + b_{7,7}) \neq 0, \quad (24)$$

can destroy the last block for eigenvalue 0 to make  $A$  invertible.

Note that the common way of adding boundaries, if the two-dimensional DFT is used for spectral analysis, makes the graph a torus, which implies six added edges in this case.

**Weighted graphs.** We concentrate in our theoretical considerations on *unweighted* directed graphs. This is justified since from Hershkowitz [40, Thm. 4.23] it follows that if an unweighted digraph is diagonalizable, then a generic weighted version of the digraph, with weights not equal to zero, is

diagonalizable as well. Indeed, consider any weighted version of the example in Fig. 1 with nonzero weights  $w_1, \dots, w_n$ . Then

$$\begin{bmatrix} 0 & w_1 & 0 & \cdots & 0 \\ 0 & 0 & w_2 & \cdots & 0 \\ \vdots & & & \ddots & \vdots \\ 0 & 0 & 0 & \cdots & w_{n-1} \\ 0 & 0 & 0 & \cdots & 0 \end{bmatrix} \quad (25)$$

has the JNF with one block shown in Fig. 1b with base change  $V = \text{diag}(1, \frac{1}{w_1}, \frac{1}{w_1 w_2}, \dots, \frac{1}{w_1 \dots w_{n-1}})$ . On the other hand, any weighted version of the directed cycle

$$\begin{bmatrix} 0 & w_1 & 0 & \cdots & 0 \\ 0 & 0 & w_2 & \cdots & 0 \\ \vdots & & & \ddots & \vdots \\ 0 & 0 & 0 & \cdots & w_{n-1} \\ w_n & 0 & 0 & \cdots & 0 \end{bmatrix} \quad (26)$$

with  $w_n \neq 0$  is diagonalizable.

If the weights happen to be not generic, which can happen, for example, if they are integer values, it is straightforward to generalize Algorithm 2 to this situation.

#### D. Destroying Jordan Blocks of Directed Laplacians

We briefly explain the straightforward extension of our approach to directed Laplacians  $L = D - A$ , where  $D$  is the matrix of outdegrees (alternatively indegrees) and  $A$  the adjacency matrix. Note that this definition is not compatible with self-loops, which are thus disallowed.

The only needed modification of Algorithm 2 is to ensure that adding an edge maintains the Laplacian structure. This means that, in addition, 1 has to be added on the main diagonal (or subtracted if an edge is removed). Thus, the perturbation  $B$  has now two entries, -1 and 1, but in the same row, so the rank is still 1 and Corollary 2 can be applied.

Note that necessarily 0 is an eigenvalue of every Laplacian with eigenvector  $(1, 1, \dots, 1)^T$ . It is also known that all Jordan blocks for eigenvalue  $\lambda = 0$  have size 1 [41]. We establish that the larger blocks (and thus for  $\lambda \neq 0$ ) can indeed be destroyed by adding edges.

**Theorem 10** Adding or deleting one edge is sufficient to destroy the largest Jordan block of a Laplacian for a chosen eigenvalue  $\lambda \neq 0$ .

**PROOF:** Let  $u_1, \dots, u_r$  and  $v_1, \dots, v_r$  be the left and right eigenvectors of the largest Jordan blocks for the eigenvalue  $\lambda \neq 0$ , respectively. Then, as in Theorem 10, (11) yields

$$0 \neq \left( \sum_{k=1}^r v_k^T \otimes u_k^T \right) \text{vec}(B) = w^T \text{vec}(B), \quad (27)$$

where  $B$  has the structure explained above. Assume this is not possible. Then, in particular, the first  $n$  elements of  $w$  are all equal, say equal to  $a \neq 0$ . From (27) we get

$$a \cdot (1, 1, \dots, 1)^T = v_{1,1} u_1^T + \dots v_{r,1} u_r^T,$$

which implies that  $(1, 1, \dots, 1)^T$  is an eigenvector for  $\lambda \neq 0$  a contradiction.  $\square$

**Example.** We consider one example.

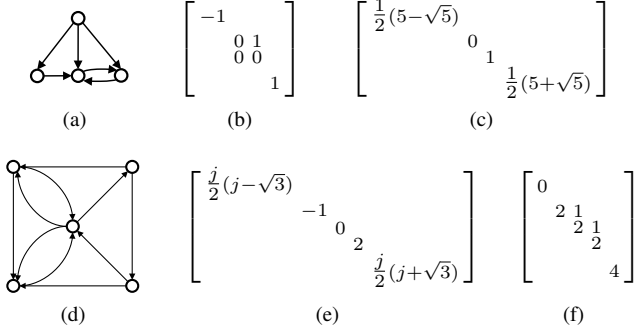


Fig. 8: Counterexamples to implications of diagonalizability of adjacency/Laplacian. From left to right: graph, adjacency Jordan structure, Laplacian Jordan structure.

*Example 11* Consider the directed Laplacian of the graph in Fig. 7. The Jordan structure is

$$\begin{bmatrix} 0 & & & & \\ 1 & 1 & & & \\ & 1 & 1 & & \\ & 0 & 1 & 2 & \\ & & & 2 & 1 & 0 \\ & & & 0 & 2 & 1 \\ & & & 0 & 0 & 2 \end{bmatrix}. \quad (28)$$

The conditions to destroy the Jordan blocks of size greater than one are

$$\begin{aligned} b_{7,1} - b_{7,4} + b_{8,1} - b_{8,4} + b_{9,1} - b_{9,4} &\neq 0, \\ b_{3,1} - b_{3,2} + b_{6,1} - b_{6,2} + b_{9,1} - b_{9,2} &\neq 0, \\ 2b_{9,1} - 2b_{9,2} - 2b_{9,4} + 2b_{9,5} &\neq 0. \end{aligned} \quad (29)$$

Hence the largest Jordan blocks to the eigenvalues 1 and 2 can be destroyed by adding the edge (9,1). Note that this does not destroy both Jordan blocks to the eigenvalue 1, since a perturbation of rank one can at most destroy one Jordan block to an eigenvalue. The condition to destroy the remaining Jordan block to the eigenvalue 1 reads

$$\frac{1}{2}(b_{3,2} + b_{3,4} + b_{6,2} + b_{6,4} + b_{7,2} - b_{7,4} + b_{8,2} - b_{8,4}) \neq 0. \quad (30)$$

Thus the choices are the same four edges as in (23) plus four additional edges.

**Adjacency matrix versus Laplacian.** In general, the diagonalizability of the adjacency matrix or Laplacian are different properties. Fig. 8 shows counterexamples for both implications.

#### IV. ALGORITHM AND IMPLEMENTATION

In this section we explain how to implement the Algorithm 2 numerically. The challenge is to achieve both numerical stability and scalability to large graphs, where the former is necessary for the latter. More concretely, we address two main challenges. First, the algorithm in Fig. 2 requires the eigenvectors of all largest Jordan blocks, but the Jordan basis is not computable for larger graphs. Second, small numerical errors can lead to the addition of unnecessary edges. Thus we need suitable heuristics.

Finally, we argue that in real-world graphs most of the non-trivial Jordan blocks are associated with the eigenvalue 0. We

exploit this observation with a special algorithm variant that enables scaling to graphs with several thousands of nodes.

We implemented our algorithms in Matlab<sup>2</sup>, which requires some additional details that we explain as well.

##### A. Numerical Algorithm: Details

We explain the additional details to make the algorithm in Fig. 2 efficiently applicable in practice.

**Eigenvectors of largest Jordan blocks.** The algorithm requires the eigenvectors of all largest Jordan blocks. In practice, we cannot determine the largest Jordan blocks via computing the JNF (except for very small graphs). Typical implementations of the eigendecomposition, as the one used in Matlab, give as output for non-diagonalizable matrices still a complete matrix of eigenvectors, in which, however, each eigenvector is usually repeated as often as the corresponding Jordan block size. Thus, as a first heuristic, we compute the pairwise angles between the spaces spanned by the eigenvectors and determining the largest group with angles very close to zero.

Since there is no certain way to obtain the eigenvectors of all largest blocks, we compute only one using the above heuristic. This means, as a second heuristic, we then aim to make only one summand in condition (11) nonzero. In the (non-generic) case that cancellation happens, i.e., the sum is zero, the guarantee of destroying a Jordan block would be lost.

Both heuristics are robust in the sense that in the worst case they add useless edges, which does not affect termination, as discussed before.

**Choice of edge.** In general, Algorithm 2 produces in each iteration several choices for the edge to add, based on the sparsity pattern of our chosen (with above heuristic)  $u$  and  $v$ . Since very small nonzero values could be rounding errors, we choose the edge corresponding to the maximal absolute value in both  $v$  and  $u$  for stability.

**Sparsity and eigenvalue 0.** An adjacency matrix can have nontrivial Jordan blocks for any eigenvalue (this can be shown using the rooted product of graphs). However, in real-world graphs and some of the random graph models commonly considered, we frequently observe the eigenvalue 0 with high multiplicity, which was also observed in [24]. This observation can be explained with Theorem 8: real-world graphs are typically sparse so it is likely that several edges are not part of any cycle, which yields a large factor  $x^m$  in the characteristic polynomial.

This observation is valuable, since it is computationally much cheaper to compute only one eigenvector to a known eigenvalue. Matlab offers the function `eigs` for this purpose. As an additional benefit, this function also has special support for sparse matrices unlike the `eig` function.

##### B. Implementation

We used the above insights and heuristics to refine Algorithm 2 into two algorithms. Algorithm 9 destroys all Jordan

<sup>2</sup>The code is available as open source at <https://github.com/bseifert-HSA/digraphSP-generalized-boundaries>.

```

function DESTROYJORDANBLOCKS(A)
   $U, V \leftarrow$  left and right eigenvectors of  $A$ 
  while  $\text{rank}(V, \epsilon_R) < n$  do
     $D \leftarrow \text{acos}(|V^T \cdot V|)$ 
     $k \leftarrow \text{argmax}_k (\#(D_{k,i} < \epsilon_D))$ 
     $(i, j) \leftarrow \text{argmax}_{i,j} (|U_{i,k}| \cdot |V_{j,k}|)$  s.t.  $A_{i,j} = 0$ 
     $A_{i,j} \leftarrow 1$ 
     $U, V \leftarrow$  right and left eigenvectors of  $A$ 
  end while
  return  $A$ 
end function

```

- ▷ Check if eigenvectors form a basis
- ▷ Pairwise angles between subspaces spanned by eigenvectors
- ▷ Index of eigenvector for largest Jordan block
- ▷ Choose edge which destroys the largest Jordan block
- ▷ Add the new edge

Fig. 9: Algorithm for obtaining a digraph with a diagonalizable adjacency matrix by destroying all Jordan blocks. In our experiments a rank tolerance  $\epsilon_R = 10^{-6}$  and an eigenspace angle tolerance  $\epsilon_D$  of one degree were used.

```

function DESTROYZEROEIGENVALUES(A)
   $D \leftarrow$  eigenvalues of  $A$ 
  while there exists  $|D_i| < \epsilon_Z$  do
     $u, v \leftarrow$  right/left eigenvector to  $D_i$ 
     $(i, j) \leftarrow \text{argmax}_{i,j} (|u_i| \cdot |v_j|)$  s.t.  $A_{i,j} = 0$ 
     $A_{i,j} \leftarrow 1$ 
     $D \leftarrow$  eigenvalues of  $A$ 
  end while
  return  $A$ 
end function

```

- ▷ Very small eigenvalues are considered zero
- ▷ Compute only one right/left eigenvector to  $D_i$
- ▷ Choose edge to be added
- ▷ Add the new edge

Fig. 10: Algorithm for removing all zero eigenvalues of a digraph. In our experiments we choose  $\epsilon_Z = 10^{-3}$  as tolerance for identifying zeros.

blocks of a digraph to obtain a diagonalizable adjacency matrix. As an optional preprocessing step, the considerable more efficient Algorithm 10 adds edges to remove all zero eigenvalues and hence yields an invertible adjacency matrix. Note that the algorithms require numerical tolerance parameters to determine which eigenvalues are 0, and which eigenvectors should be considered as collinear or equal.

**DestroyJordanBlocks.** From the above considerations we can now derive the numerical Algorithm 9. First we calculate the left and right eigenmatrices  $U, V$  of the adjacency matrix  $A$ . While  $A$  is not diagonalizable, which we check by testing if  $V$  is rank-deficient, we destroy iteratively the Jordan blocks. For this we use our heuristic and first calculate all the angles  $D$  between the subspaces spanned by the elements of  $V$ . Then we obtain the eigenvector, which most likely corresponds to the largest Jordan block, by finding the index  $k$  for which most entries of  $D$  are approximately zero. To find the edge, we maximize over the product of the entries of the left and right eigenvectors  $|U_{i,k}| \cdot |V_{j,k}|$  under the constraint that  $A_{i,j} = 0$ . The case of the random edge in Algorithm 2 occurs here if  $A_{i,j} = 1$  whenever the product is  $> 0$ , i.e., if the maximum is zero.

For the implementation of Algorithm 9 in Matlab we use the `eig` function with the `nobalance` option. With these options, Algorithm 9 is applicable to all matrix sizes for which one can calculate the complete eigendecomposition of a full matrix.

For the computation of  $\text{rank}(V)$ , Matlab requires a tolerance, for which we chose  $\epsilon_R = 10^{-6}$ , meaning that the smallest singular value fulfills  $\sigma_{\min} > 10^{-6}$ . In [22] this condition was used to define a Fourier basis as numerical stable. Thus our constructed bases are stable in the same sense. As tolerance  $\epsilon_D$  to identify two eigenvectors we observed that an angle of one degree is a good choice.

**DestroyZeroEigenvalues.** Algorithm 10 destroys all zero eigenvalues. Here we first calculate the *eigenvalues* of the adjacency matrix  $A$ . As long as an eigenvalue is approximately zero, we calculate an associated left and right eigenvector. Then we destroy the Jordan block to that eigenvalue similar as in Algorithm 9.

We implement Algorithm 10 using sparse matrices in the compressed sparse row (CSR) format and use the Matlab function `eigs` to find one eigenvector to the numerical eigenvalue zero and destroy the corresponding Jordan block. Thus, Algorithm 10 scales to all matrix sizes for which one can calculate one eigenvector for a sparse matrix. In our experiments we consider eigenvalues as zero if their absolute value is  $\leq \epsilon_Z = 10^{-3}$ .

Since we argued already that in real-world graphs typically many Jordan blocks are associated to the eigenvalue 0, one can obtain a significant speedup by first removing all zeros from the eigenvalues of a graph using Algorithm 10 and then, afterwards, applying the more costly Algorithm 9 to destroy the remaining Jordan blocks.

**Robustness.** We note that our algorithms yield an inherent robustness property: our parameter settings ensure that the final digraph obtained does not have very small eigenvalues, does not have almost collinear eigenspaces, and produces a numerically stable Fourier basis.

**Complexity.** In the implementation of `DestroyZeroEigenvalues` we use the sparse CSR matrix format, which requires space of size  $O(\max(n, m))$ , where  $n$  is the size of the matrix and  $m$  the number of nonzero entries [42]. Updating the adjacency matrix with a new edge requires  $O(m)$  operations. `eigs` calculates an eigenvector to the eigenvalue zero in time  $O(nk^2)$  using a Krylov-Schur algorithm [43];  $k$  depends on the rate of convergence which is hard to estimate beforehand,

The implementation of `DestroyJordanBlocks` relies on full

matrices and hence the required storage is  $O(n^2)$ . The complexity of computing the complete eigendecomposition and the pairwise angles is  $O(n^3)$ .

## V. EXPERIMENTS AND APPLICATIONS

We evaluate our proposed algorithm and implementation with two kinds of experiments. First, we apply our algorithm to a set of random and real-world graphs to make them diagonalizable (and possibly invertible) and investigate the results. Then we show a Wiener filter as prototypical application that is enabled by using our approach that first establishes a complete basis of eigenvectors. Finally, we consider also the case of a Laplacian to demonstrate that our approach is equally applicable.

The experiments in this section, unless stated otherwise, were performed on a computer with an Intel Core i9-9880H CPU and 32 GB of RAM.

### A. Computing generalized boundary conditions

**Random digraphs.** In our first experiment we apply our algorithm DestroyJordanBlocks in Fig. 9 to four different classes of random digraphs [44]. We briefly recall their properties.

The Erdős–Rényi model creates homogeneous digraphs in the sense that the degree distribution of the nodes decays symmetrically from the mean degree, the average path length increases as the graph size increases, and its clustering coefficient reduces as the graph size increases.

The Watts–Strogatz model leads to small-world digraphs which means they have large clustering coefficients, unlike the Erdős–Rényi random graphs.

The Barabási–Albert model yields scale-free digraphs in the sense that their degree distribution is very inhomogeneous, which means they contain a large numbers of nodes with small degree and a only a few hubs with large degree.

The fourth model is Klemm–Eguíluz, which combines the small-world property of the Watts–Strogatz model with the scale-freeness of the Barabási–Albert model. Since it is conjectured that real-world networks are scale-free and small-world, these graphs may be particularly realistic.

For each model we generated 100 random weakly connected graphs<sup>3</sup> with 500 nodes. We set the model parameters to obtain an average of about 5000 edges in each case. For the Erdős–Rényi model we choose a success probability of connecting two nodes of 0.02. We created Watts–Strogatz model graphs with 10 edges to each node in the initial ring lattice and a rewiring probability of 0.001. The Barabási–Albert model got as parameters a seed size of 10 and an average degree of the nodes of 10. Finally we used the Klemm–Eguíluz model with seed size 5 and a probability of connecting to non-active nodes of 0.1. The parameters are explained in [44].

For Erdős–Rényi, all generated graphs were diagonalizable. For the other models we summarize the results of applying DestroyJordanBlocks in Table. I. The table reports the minimum, median, and maximum number of edges added to make

	min		median		max	
	edges	time	edges	time	edges	time
Watts–Strogatz	0	0.2s	1	0.5s	3	1.3s
Barabási–Albert	36	4.4s	44	10s	55	31s
Klemm–Eguíluz	10	2.2s	27	6s	47	9s

TABLE I: Edges added and runtime of DestroyJordanBlocks for three different random graph models with 500 nodes and approximately 5000 edges.

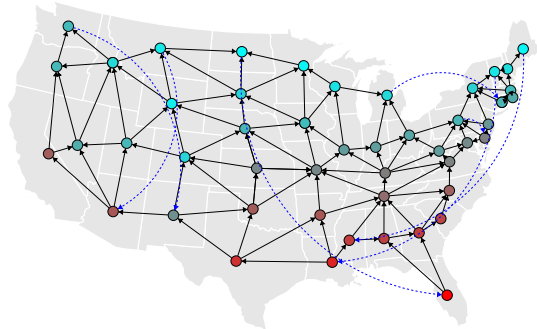


Fig. 11: The USA graph. The 7 new edges added by DestroyJordanBlocks are shown as dashed blue.

them diagonalizable and the runtime to do so. The first main observation is that our algorithm works in each case and with a runtime that is easily acceptable for a one-time preprocessing step. For Watts–Strogatz very few edges are sufficient in all cases, whereas for the other two up to 1% additional edges may be needed in the worst case.

Next, we consider three real-world graphs.

**USA graph.** First, we consider a small digraph consisting of the 48 contiguous US states with edges going from lower to higher latitude (see Fig. 11) that has been a popular use case in several publications (e.g., [21], [26]). The graph consists of 48 nodes and 105 edges and is an extreme case since it is acyclic, i.e., only has the eigenvalue 0, with 7 Jordan blocks of sizes 13, 10, 9, 5, 5, 4, 2, respectively. Application of DestroyJordanBlocks yields (the minimal needed number of) 7 added edges shown in Fig. 11 dashed in blue. The eigenvalues of the modified graph are shown in Fig. 12. They are all simple eigenvalues, and well-separated, which is ideal for any subsequent GSP analysis. Further, Fig. 13 shows the angles between (spaces generated by the) eigenvectors. On the left for the Jordan basis of the original USA graph (which for this size is still computable) and on the right for the eigenbasis of the modified graph. The basis is not far from orthogonal, a property that will become more pronounced for the larger graphs considered next.

**Manhattan taxi graph.** Next we demonstrate that our algorithm can process large-scale graphs that are particular challenging in numerical stability. First we consider the Manhattan taxi graph used in [45], [22]<sup>4</sup> and shown in Fig. 14. The graph consists of 5464 nodes, each representing a spatial

<sup>3</sup>If a graph is not weakly connected the components can be processed separately.

<sup>4</sup>The graph and the graph signal is based on data available at <https://www1.nyc.gov/site/tlc/about/tlc-trip-record-data.page>

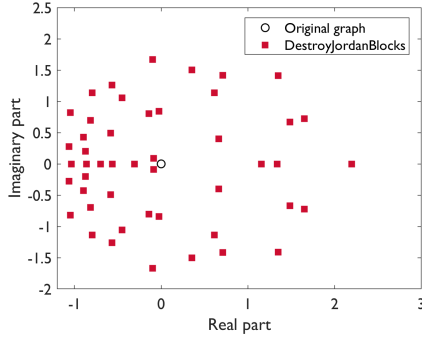


Fig. 12: The eigenvalues of the USA graph (black circle), and after making it diagonalizable (red squares).

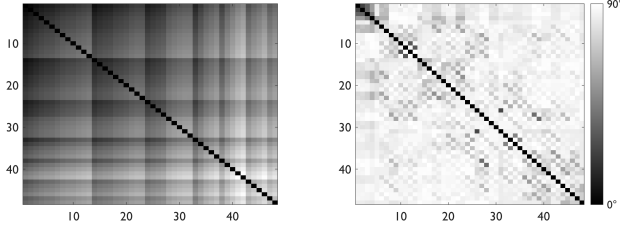


Fig. 13: The angles between the computed generalized eigenvectors of the original USA graph (left) and the angles between the computed eigenvectors of the USA graph with the additional edges (right).

location at the intersection of streets or along a street. A directed edge means that traffic is allowed to directly move from one node to the other. The total number of edges in the graph is 11568.

Because of the large scale and rank deficiency, as explained in Section IV-B, we first apply DestroyZeroEigenvalues in Fig. 10 to first remove all zero eigenvalues, which took 2.3 minutes and added 772 edges (about 6.7%). Then we applied DestroyJordanBlocks in Fig. 9, which added another 1 edge in 2.5 minutes for a total processing time of about 5 minutes. Our algorithm guarantees that the resulting graph has a computed eigenmatrix with full rank (with tolerance  $\sigma_{\min} \geq \epsilon_R = 10^{-6}$ ), and a minimal angle between computed eigenvectors of  $\epsilon_D \geq$  one degree. However, Fig. 15 shows that the eigenbasis is

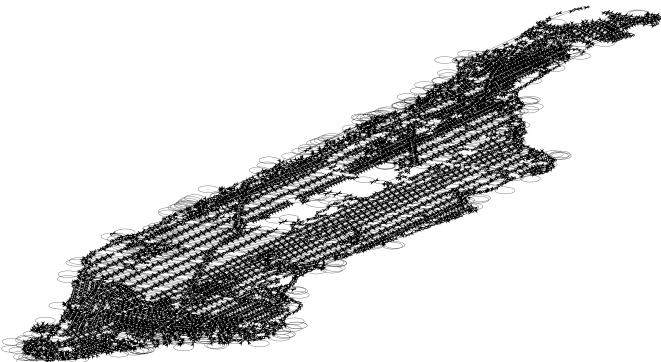


Fig. 14: The Manhattan graph with 5464 nodes.

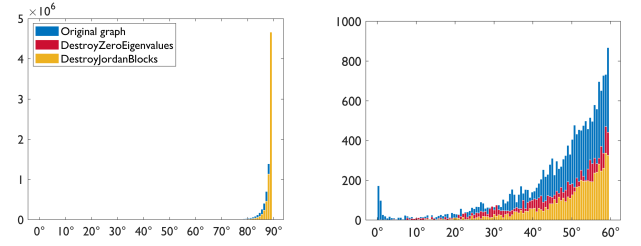


Fig. 15: Manhattan graph: The histogram of all  $5464^2$  angles between the spaces spanned by the computed eigenvectors: for all angles (left), and zoomed in on angles  $\leq 60$  degrees (right).

even very close orthogonal. It is also numerically stable:  $\sigma_{\min} = 0.0017$ ,  $\sigma_{\max} = 4.9158$ , i.e., the condition number is  $\kappa = \sigma_{\max}/\sigma_{\min} = 2892$ , which means we can compute a valid Fourier transform by inversion<sup>5</sup>.

To show the gain in computational complexity, we also applied only DestroyJordanBlocks from Fig. 9. For this experiment we used a computer with Intel Xeon CPU E5-2660, 2.2 GHz with 128 GB of RAM. The algorithm added 243 additional edges within 19 hours. Even though the number of edges added differs significantly, the eigenspace angle distribution for both approaches turned out very similar, meaning in both cases one obtains an almost orthogonal graph Fourier transform. The eigenbasis obtained by applying only DestroyJordanBlocks is slightly less stable:  $\sigma_{\min} = 0.0006$ ,  $\sigma_{\max} = 4.897$  for a condition number of  $\kappa = 7802$ . Note that when using only DestroyJordanBlocks, the adjacency matrix still has eigenvalue zero with a high (namely 536) multiplicity.

In the following we consider only the previous modified graph obtained with the fast method that combines both algorithms.

Fig. 16a shows that the eigenvalues of the modified graph lie in a similar range as those of the original graph, except for those near zero that we destroyed.

Basis vectors  $v$  can be ordered by total variation  $TV_A$  (see (5)) w.r.t. the adjacency matrix  $A$ . For an eigenvector  $v$  with  $\|v\|_1 = 1$  and eigenvalue  $\lambda$ ,  $TV_A(v) = |1 - \lambda/\lambda_{\max}|$ . We noted earlier (Lemma 6) that the eigenvectors  $v$  of our modified graph  $(A+B)$  are, in a sense, approximate eigenvectors for the original  $A$ . Here we compare the total variations  $TV_{A+B}(v)$  and  $TV_A(v)$  of the eigenbasis of  $A+B$  when used as basis for  $A$ .

Fig. 16b plots  $TV_A(v)$  against  $TV_{A+B}(v)$ . Even though about 6.5% of edges were added, the total variations are almost equal. This means that our method preserved the ordering of frequencies and thus the notion of low and high frequency. Thus, for example, a low-pass filter designed for the diagonalizable graph  $A+B$  will be a low pass filter for the original  $A$ .

We also show the distribution curve of the total variations in Fig. 16c. Interestingly, it is similar to the curve in [22,

<sup>5</sup>If the condition number is  $\kappa$ , about  $\log_{10} \kappa$  decimal digits of precision are lost when inverting the matrix in floating point [46, p. 95]. Here it is only 3 digits out of 16 available in double precision.

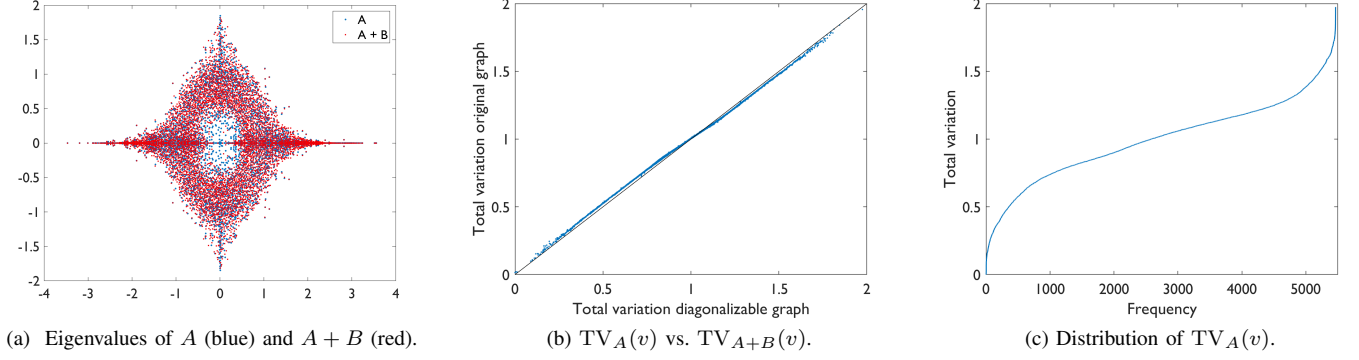


Fig. 16: Properties of the eigenvalues and eigenvectors  $v$  of the modified Manhattan graph  $A + B$ .



Fig. 17: The graph signal of averaged hourly taxi rides on the Manhattan graph.

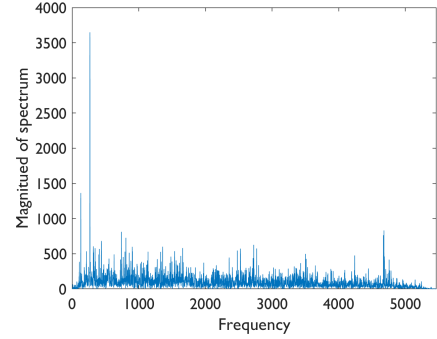


Fig. 18: The spectrum of the Manhattan graph signal. The frequencies are ordered by total variation.

Fig. 16], even though a very different approximation method was used.

The work in [45] used as signal on the Manhattan graph the number of hourly taxi rides starting from each node. Similarly, we take the number of taxi rides averaged over the first half of 2016. The obtained graph signal is shown in Fig. 17.

We apply the graph Fourier transform for the graph we obtained by applying `DestroyZeroEigenvalues` and `DestroyJordanBlocks` to the Manhattan graph to this signal. For this, we sorted the eigenvectors with respect to total variation and normalized them to  $\|v\|_2 = 1$ . The obtained magnitude signal spectrum is shown in Fig. 18.

**Citation graph.** As second large real-world graph we use the arXiv HEP-PH citation graph released in [47]<sup>6</sup>. For our experiments we used a weakly connected subgraph with 4989 vertices and 17840 edges shown in Fig. 19, where the nodes are vertically placed by publication time.

As a citation graph this graph is very close to being acyclic and thus has almost all eigenvalues 0, i.e., it is particularly challenging.

As before, we first apply `DestroyZeroEigenvalues` in Fig. 10 to remove all eigenvalue zeroes, which took 9.5 minutes and added 1890 edges (about 10.5%). Using `DestroyJordanBlocks` then added another 21 edges in 22 minutes and gives the

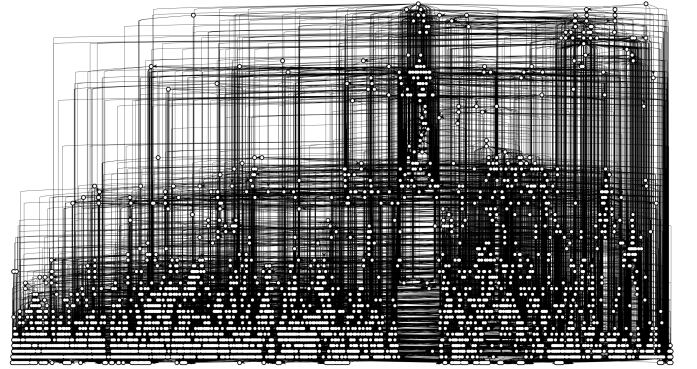


Fig. 19: A citation graph with 4989 nodes.

usual guarantees on the minimal angle between the computed eigenspaces. However, Fig. 20 shows that, as for the Manhattan graph, the eigenbasis is even almost orthogonal. The obtained Fourier basis, with  $\|v\|_2 = 1$ , is again numerically stable:  $\sigma_{\min} = 0.0026$ ,  $\sigma_{\max} = 5.1847$ , for a condition number of  $\kappa = 1994.1$ .

As for the Manhattan graph, Fig. 21 plots  $TV_A(v)$  against  $TV_{A+B}(v)$ . Even though about 10% of edges were added, they are close to equal and very close to order preserving.

<sup>6</sup>The graph is available online at <https://snap.stanford.edu/data/cit-HepPh.html>

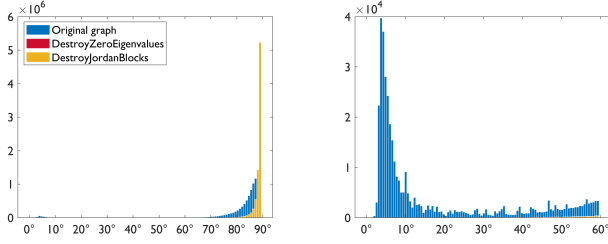


Fig. 20: Citation graph: The histogram of all  $4989^2$  angles between the spaces spanned by the computed eigenvectors for the citation graph: for all angles (left), and zoomed in on angles  $\leq 60$  degrees (right).

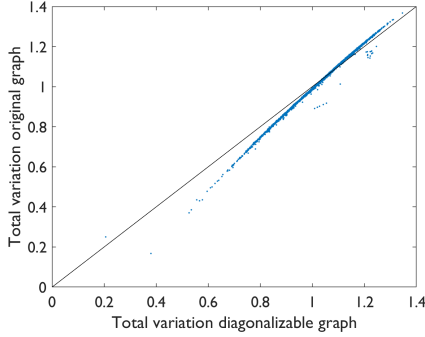


Fig. 21:  $TV_A(v)$  vs.  $TV_{A+B}(v)$  for the eigenvectors  $v$  of  $A + B$ .

### B. Wiener filtering with energy preserving shift

The work in [48] introduced an energy-preserving shift for graphs and digraphs but required the adjacency matrix to be diagonalizable. We show that our work can be used as a preprocessing step to establish this property to then enable further SP. As example, we use the generalization of Wiener filtering to graphs show-cased in [48]. First, we briefly provide background from [48].

**Energy-preserving shift.** Let  $A = VDV^{-1}$  with  $D$  diagonal and let  $\Lambda_e = \text{diag}(\lambda_{e_1}, \dots, \lambda_{e_N})$ , with  $\lambda_{e_k} = e^{-2j\pi(k-1)/n}$ . The energy-preserving graph shift is then defined as

$$A_e = V\Lambda_e V^{-1}. \quad (31)$$

Thus,  $\|\mathcal{F}s\| = \|\mathcal{F}(A_e s)\|$  and  $n$  applications to a signal reproduce the original:  $A_e^n x = x$ . If the eigenvalues of  $A$  are all simple,  $A_e$  is a polynomial in  $A$ , i.e., a filter.

**Graph Wiener filter.** Consider a graph signal  $x$  and a noisy measurement of the signal  $y = x + n$ . The graph Wiener filter of order  $L$  has the form

$$H = \sum_{k=0}^{L-1} h_k A_e^k, \quad (32)$$

where the filter coefficients  $h$  are found by solving

$$\min_h \|Bh - x\|_2^2, \quad \text{with } B = [y \ A_e y \ \dots \ A_e^{L-1} y]. \quad (33)$$

Using  $R_{y,y}(\ell, m) = y^H(A_e^\ell)^H A_e^m y$  as definition for autocorrelation of the graph signal  $y$ , and  $r_{x,y}(\ell) = y^H(A_e^\ell)^H x$  as

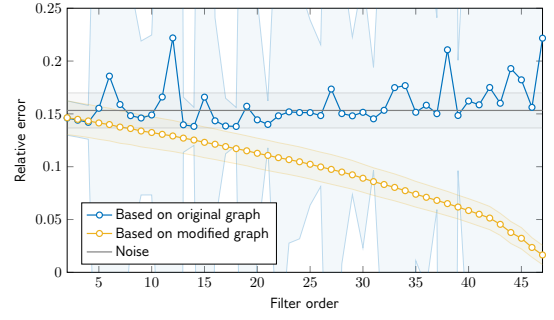


Fig. 22: The relative reconstruction error  $\|x - d\|/\|x\|$  of the Wiener filtered noisy signal  $d$  compared the original signal  $x$ , for different filter orders and energy-preserving shifts based on the adjacency matrix of the original graph and our modified graph. We used normally distributed noise with mean 0 and standard deviation 10. The average over 1000 noise simulations is shown as thick line and the standard deviation as shaded area in the respective colors.

definition of the cross-correlation between the graph signals  $x$ , yields the linear equation

$$R_{y,y}h = r_{x,y} \quad (34)$$

for the coefficients of the Wiener filter. Note that the powers of  $A_e$  can be computed efficiently using  $A_e^k = V\Lambda_e^k V^{-1}$ .

**Small graph signal.** Since in [48] a random graph was used to evaluate the graph Wiener filter, we use the USA graph in Fig. 11 for our experiments. As graph signal we used, similar to [21], [26], the average monthly temperature of each state<sup>7</sup>. Then we added, over 1000 simulations, normally distributed noise with zero mean and standard deviation of 10 to the signal, leading to a signal-to-noise ratio of  $14.4 \pm 0.9$  decibel.

**Small graph results.** Fig. 22 shows the relative reconstruction error, as function of the filter order, for the graph Wiener filtered signal. The filter was designed with our modified graph that ensures diagonalizability. The qualitative behavior is as expected based on the results in [48]. Designing the Wiener filter based on the original graph and its Jordan basis fails (and was also not proposed in [48]).

**Large graph results.** The experiments in [48] only considered a graph with 40 nodes. Here, we repeat the previous experiment with the large scale Manhattan graph signal in Fig. 17 with added noise. Since the JNF is (by far) not computable in this case (and the method also did not work with the Jordan basis in Fig. 22) we only show the results for the modified graph after applying DestroyZeroEigenvalues and DestroyJordanBlocks and get a roughly similar behavior as before. Due to the high computational cost we show only one run and thus no standard deviation.

In summary, using our method as preprocessing step makes the design of Wiener filters from [48] applicable to non-diagonalizable digraphs.

<sup>7</sup>Available on <https://www.currentresults.com/Weather/US/average-annual-state-temperatures.php>

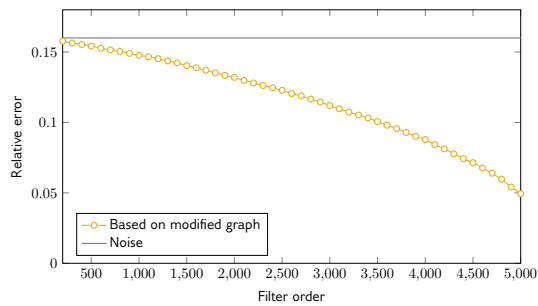


Fig. 23: The relative reconstruction error  $\|x - d\|/\|x\|$  of the Wiener filtered noisy signal  $d$  to the original Manhattan graph signal  $x$ . In this experiment we added normally distributed noise with mean 0 and standard deviation 0.5.

	min		median		max	
	edges	time	edges	time	edges	time
Watts-Strogatz	0	0.1s	0	0.12s	3	0.61s
Barabási-Albert	27	3.3s	40	4.8s	55	6.9s
Klemm-Eguíluz	3	0.4s	12	1.6s	52	5.5s

TABLE II: Edges added and runtime of DestroyJordanBlocks for three different random graph models with 500 nodes and approximately 5000 edges.

### C. Laplacian

In this section we repeat some of the above experiments for the Laplacian instead of the adjacency matrix, to demonstrate that our algorithm is equally applicable with minor modifications. For  $D$  we use the in-degrees in all experiments. We have to slightly adjust DestroyJordanBlocks in Fig. 9, replacing the condition  $u_i \cdot v_j \neq 0$  with  $v_j(u_j - u_i) \neq 0$ . Note that there is no analogue of the algorithm from Fig. 10 for the Laplacian, as no particular eigenvalue has a distinguished significance and zero is always an eigenvalue and thus cannot be destroyed. For example, in directed acyclic graphs Jordan blocks can only appear only if there are nodes with the same number of incoming edges.

We also remind the reader that diagonalizability of  $A$  and  $L = D - A$  are different properties (see Fig. 8) in general.

**Random graphs.** As for the experiment with the adjacency matrix, we generate 100 random digraphs for each of the random digraph models. The Laplacians of the Erdős-Rényi random graphs are again all diagonalizable. For the other three types of random digraphs the results are shown in Table II. The overall behavior is similar as before in Table I.

**USA graph.** The Jordan structure for the Laplacian of the USA graph is shown in Table III. To obtain a diagonalizable Laplacian on the USA graph our algorithm adds 6 additional edges (one more than the theoretical minimum of 5), shown in Fig. 24. The eigenvalues before and after adding the edges are shown in Fig. 25.

**Manhattan taxi graph.** We apply DestroyJordanBlocks to the Laplacian of the Manhattan graph. The algorithm added 596 new edges within 12 hours. The angles between the computed eigenvectors before and after adding the edges are shown in Fig. 26, i.e., the Fourier basis is close to orthogonal.

Eigenvalue	Block sizes
0	1,1,1,1
1	4,3,2,1,1,1
2	4,2,1,1,1
3	8,4,3,2,2
4	2
5	2

TABLE III: Jordan block sizes for Laplacian of the USA graph.

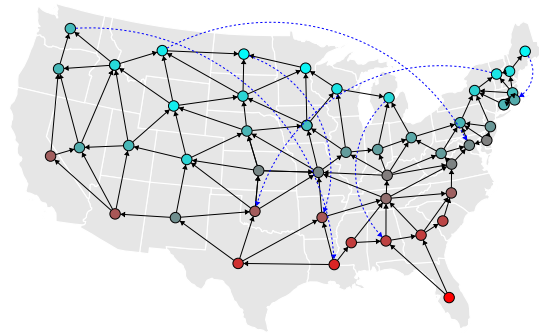


Fig. 24: The USA graph. The 6 new edges added by DestroyJordanBlocks for the Laplacian are shown as dashed blue.

The eigenvalues  $L + B$  are in the same range as those of  $L$  (Fig. 27).

## VI. CONCLUSION

We presented a practical and scalable solution to the challenging problem of designing a suitable Fourier basis in the case of non-diagonalizable shifts and filters in digraph signal processing. The basic idea was to add edges, i.e., slightly perturb the adjacency or Laplacian matrix to enforce this property. Then the Fourier basis and transform of the modified graph are used for the original graph. Equivalently, our method can be seen as a way to construct an approximate, numerically stable eigenbasis and associated approximate Fourier transform that are still associated with an intuitive notion of shift in the graph domain. We showed that the method even works for directed acyclic graphs, which only have the eigenvalue zero.

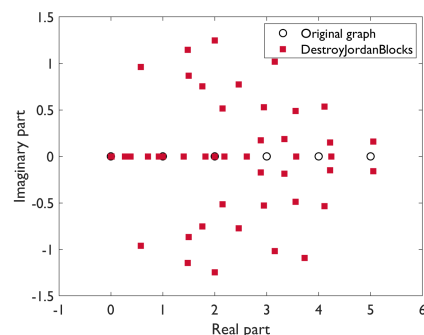


Fig. 25: The Laplacian eigenvalues of the USA graph (black circle), and after making it diagonalizable (red squares).

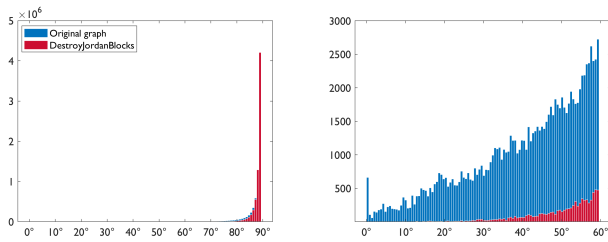


Fig. 26: Manhattan graph: The histogram of all  $5464^2$  angles between the spaces spanned by the computed eigenvectors of the Laplacian: for all angles (left), and zoomed in on angles  $\leq 60$  degrees (right).

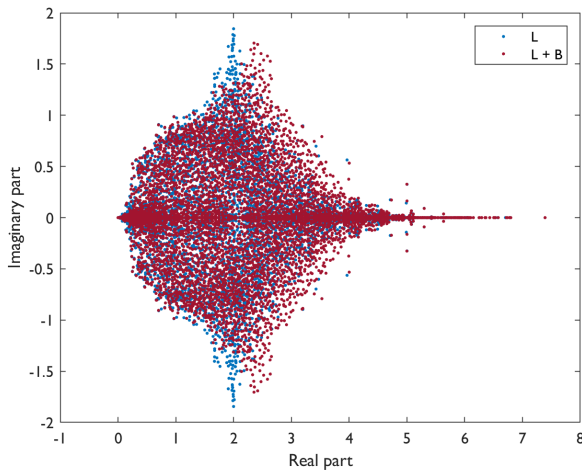


Fig. 27: Eigenvalues of the modified Laplacian of the Manhattan graph  $L + B$ .

Our method has more general potential uses to establish other desirable properties. Examples that we showed in the paper include invertibility or simple eigenvalues only for the graph shift, properties that are required or desirable for certain applications. It is intriguing, and invites further investigation, that the added edges must add cycles in the graph, thus generalizing the concept of cyclic boundary conditions. Also intriguing is that the Fourier bases obtained seem to be close to orthogonal and that they seem to maintain the total variation and its ordering with respect to the original graph. Finally, we would like to stress that the implementation of our method copes well with the inherent numerical instability of eigenvalue computations and scales to several thousands nodes.

## REFERENCES

- [1] I. Jablonski, "Graph Signal Processing in Applications to Sensor Networks, Smart Grids, and Smart Cities," *IEEE Sensors Journal*, vol. 17, no. 23, pp. 7659–7666, 2017.
- [2] H. Padole, S. D. Joshi, and T. K. Gandhi, "Early Detection of Alzheimer's Disease using Graph Signal Processing on Neuroimaging Data," in *2018 2nd European Conference on Electrical Engineering and Computer Science (EECS)*, Dec 2018, pp. 302–306.
- [3] A. Pirayre, C. Couprie, F. Bidard, L. Duval, and J.-C. Pesquet, "BRANE Cut: Biologically-related a priori network enhancement with graph cuts for gene regulatory network inference," *BMC Bioinf.*, vol. 16, no. 1, pp. 368, 2015.
- [4] D. Thanou, P.A. Chou, and P. Frossard, "Graph-Based Compression of Dynamic 3D Point Cloud Sequences," *IEEE Trans. Image Process.*, vol. 25, no. 4, pp. 1765–1778, 2016.
- [5] W. Huang, A.G. Marques, and A. Ribeiro, "Collaborative filtering via graph signal processing," in *Proc. 25th Eur. Signal Process. Conf. (EUSIPCO)*, 2017, pp. 1094–1098.
- [6] A. Ortega, P. Frossard, J. Kovacevic, J.M.F. Moura, and P. Vandergheynst, "Graph Signal Processing: Overview, Challenges, and Applications," *Proc. IEEE*, vol. 106, no. 5, pp. 808–828, 2018.
- [7] D.I. Shuman, S.K. Narang, P. Frossard, A. Ortega, and P. Vandergheynst, "The emerging field of signal processing on graphs: Extending high-dimensional data analysis to networks and other irregular domains," *IEEE Signal Process. Mag.*, vol. 30, no. 3, pp. 83–98, 2013.
- [8] A. Sandryhaila and J.M.F. Moura, "Discrete Signal Processing on Graphs," *IEEE Trans. Signal Process.*, vol. 61, no. 7, pp. 1644–1656, 2013.
- [9] M. Püschel and J.M.F. Moura, "Algebraic Signal Processing Theory: Foundation and 1-D Time," *Signal Processing, IEEE Trans.*, vol. 56, no. 8, pp. 3572–3585, 2008.
- [10] J. Dunne and P. E. Butterworth, "Spectral techniques in argumentation framework analysis," in *Computational Models of Argument: Proceedings of COMMA*, 2016, pp. 167–178.
- [11] J.A. Yorke and W.N. Anderson, "Predatory-prey patterns," *PNAS*, vol. 70, no. 7, pp. 2069–2071, 1973.
- [12] C.K. Chui, H.N. Mhaskar, and X. Zhuang, "Representation of functions on big data associated with directed graphs," *Applied and Computational Harmonic Analysis*, vol. 44, no. 1, pp. 165–188, 2018.
- [13] H. Kwak, C. Lee, H. Park, and S. Moon, "What is twitter, a social network or a news media?," in *Proceedings of the 19th international conference on World Wide Web*, 2010, pp. 591–600.
- [14] J.O. Kephart and S.R. White, "Directed-graph epidemiological models of computer viruses," *Computation: the micro and the macro view*, pp. 71–102, 1992.
- [15] A. Sandryhaila and J.M.F. Moura, "Discrete Signal Processing on Graphs: Frequency Analysis," *IEEE Trans. Signal Process.*, vol. 62, no. 12, pp. 3042–3054, 2014.
- [16] T. Beelen and P. Van Dooren, "Computational aspects of the Jordan canonical form," in *Reliable Numerical Computation*, Cox and Hammarling, Eds., pp. 57–72. Clarendon, 1990.
- [17] M. M. Bronstein, J. Bruna, Y. LeCun, A. Szlam, and P. Vandergheynst, "Geometric Deep Learning: Going beyond Euclidean data," *IEEE Signal Processing Magazine*, vol. 34, no. 4, pp. 18–42, 2017.
- [18] J. Moro and F. M. Dopico, "Low rank perturbation of Jordan structure," *SIAM J. Matrix Anal. Appl.*, vol. 25, no. 2, pp. 495–506, 2003.
- [19] S. Sardellitti, S. Barbarossa, and P. di Lorenzo, "On the Graph Fourier Transform for Directed Graphs," *IEEE J. Sel. Topics Signal Process.*, vol. 11, no. 6, pp. 796–811, 2017.
- [20] R. Shafipour, A. Khodabakhsh, G. Mateos, and E. Nikolova, "Digraph Fourier Transform via Spectral Dispersion Minimization," in *Proc. IEEE International Conference on Acoustics, Speech and Signal Processing (ICASSP)*, April 2018, pp. 6284–6288.
- [21] R. Shafipour, A. Khodabakhsh, G. Mateos, and E. Nikolova, "A Directed Graph Fourier Transform with Spread Frequency Components," *IEEE Trans. on Signal Processing*, vol. 67, no. 4, pp. 946–960, 2019.
- [22] J. Domingos and J.M.F. Moura, "Graph Fourier Transform: A Stable Approximation," *IEEE Trans. on Signal Processing*, vol. 68, pp. 4422–4437, 2020.
- [23] J. A. Deri and J. M. F. Moura, "Spectral Projector-Based Graph Fourier Transforms," *IEEE Sel. Topics Signal Process.*, vol. 11, no. 6, pp. 785–795, 2017.
- [24] J. A. Deri and J. M. F. Moura, "Agile Inexact Methods for Spectral Projector-Based Graph Fourier Transforms," arXiv:1701.02851, 2017.
- [25] J. A. Deri and J. M. F. Moura, "New York City Taxi Analysis with Graph Signal Processing," in *Proc. IEEE Global Conf. Inf. Process.*, December 2016, pp. 1275–1279.
- [26] S. Furutani, T. Shibahara, M. Akiyama, K. Hato, and M. Aida, "Graph Signal Processing for Directed Graphs based on the Hermitian Laplacian," in *Proc. European Conference on Machine Learning and Principles and Practice of Knowledge Discovery in Databases (ECMLPKDD)*, 2019.
- [27] R. Singh, A. Chakraborty, and B. Manoj, "Graph Fourier transform based on directed Laplacian," in *Proc. IEEE Int. Conf. Signal Process. Commun.*, 2016, pp. 1–5.
- [28] F. Bauer, "Normalized graph Laplacians for directed graphs," *Linear Algebra and its Applications*, vol. 436, no. 11, pp. 4193–4222, 2012.

- [29] P. Misiakos, C. Wendler, and M. Püschel, "Diagonalizable Shift and Filters for Directed Graphs Based on the Jordan-Chevalley Decomposition," in *Proc. IEEE International Conference on Acoustics, Speech and Signal Processing (ICASSP)*, 2020, to appear.
- [30] R. M. Mersereau, "The processing of hexagonally sampled two-dimensional signals," *Proc. IEEE*, vol. 67, pp. 930–949, 1979.
- [31] M. Püschel and M. Rötteler, "Fourier transform for the directed quincunx lattice," in *Proc. IEEE International Conference on Acoustics, Speech, and Signal Processing (ICASSP)*, March 2005, vol. 4, pp. 401–404.
- [32] M. Hein, J. Audibert, and U. von Luxburg, "Graph Laplacians and their convergence on random neighborhood graphs," *Journal of Machine Learning Research*, vol. 8, pp. 1325–1368, 2007.
- [33] F. Chung, "Laplacians and the Cheeger inequality for directed graphs," *Ann. Combinatorics*, vol. 9, no. 1, pp. 1–19, 2005.
- [34] A. Shubin, "Discrete magnetic Laplacian," *Comm. Math. Phys.*, vol. 164, pp. 259–275, 1994.
- [35] L. Hörmander and A. Melin, "A remark on perturbations of compact operators," *Math. Scand.*, vol. 75, pp. 255–262, 1994.
- [36] S. V. Savchenko, "On the change in the spectral properties of a matrix under perturbations of sufficiently low rank," *Funcional Analysis and Its Applications*, vol. 38, no. 1, pp. 69–71, 2004.
- [37] W. Kahan, B.N. Parlett, and E. Jiang, "Residual bounds on approximate eigensystems of nonnormal matrices," *SIAM J. Numer. Anal.*, vol. 19, pp. 470–484, 1982.
- [38] A. C.M. Ran and M. Wojtylak, "Eigenvalues of rank one perturbations of unstructured matrices," *Linear Algebra and its Applications*, vol. 437, pp. 589–600, 2012.
- [39] C. Coates, "Flow-Graph Solutions of Linear Algebraic Equations," *IRE Transactions on Circuit Theory*, vol. 6, no. 2, pp. 170–187, 1959.
- [40] D. Hershkowitz, "The relation between the Jordan structure of a matrix and its graph," *Linear Algebra and its Applications*, vol. 184, pp. 55–69, 1993.
- [41] J. S. Caughman and J. J. P. Veerman, "Kernels of directed graph laplacians," *The Electronic Journal of Combinatorics*, vol. 13, no. 1, 2006.
- [42] J.R. Gilbert, C. Moler, and R. Schreiber, "Sparse Matrices in Matlab: Design and Implementation," *SIAM J. Matrix Anal. Appl.*, vol. 13, no. 1, pp. 333–356, 1992.
- [43] G. W. Stewart, "A Krylov-Schur Algorithm for Large Eigenproblems," *SIAM J. Matrix Anal. Appl.*, vol. 23, no. 3, pp. 601–614, 2001.
- [44] B.J. Pettejohn, M.W. Berryman, and M.D. McDonnell, "Methods for generating complex networks with selected structural properties for simulations: A review and tutorial for neuroscientists," *Front. Comput. Neurosci.*, vol. 5, pp. 11, 2011.
- [45] Y. Li and J.M.F. Moura, "Forecaster: A Graph Transformer for Forecasting Spatial and Time-Dependent Data," in *Proc. 24th European Conference on Artificial Intelligence - ECAI*, 2020.
- [46] L. N. Trefethen and D. Bau, *Numerical Linear Algebra*, SIAM, 1997.
- [47] J. Gehrke, P. Ginsparg, and J.M. Kleinberg, "Overview of the 2003 KDD Cup," *SIGKDD Explorations*, vol. 5, no. 2, pp. 149–151, 2003.
- [48] A. Gavili and X.-P. Zhang, "On the Shift Operator, Graph Frequency, and Optimal Filtering in Graph Signal Processing," *IEEE Trans. Sign. Proc.*, vol. 65, no. 23, pp. 6303 – 6318, 2017.